Supporting Information

Cerium partial fluoridation efficiently promoted Pd nanoparticles for formic acid oxidation

Yajing Xie[a], Dongze Li[a], Yun Yang[b], Shuli Wang[a], Ligang Feng*[a]

[a] School of Chemistry and Chemical Engineering, Yangzhou University, Yangzhou, 225002, P.R China. E-mail: ligang.feng@yzu.edu.cn, fenglg11@gmail.com

[b] Nanomaterials and Chemistry Key Laboratory, Wenzhou University, Wenzhou, China. E-mail: bachier@163.com

1. Experimental section

1.1 Materials

All reagents were used as received without further purification. Sodium hydroxide concentrated sulfuric acid, ethylene glycol, and pure formic acid were purchased from Beijing Chemical Works. Palladium (II) chloride was bought from Sinopharm Chemical Reagent Co Ltd. Cerium (III) nitrate hexahydrate and ammonium fluoride. Vulcan XC-72 carbon black was purchased from the Cabot Co. Nafion (5 wt.%) was purchased from Sigma-Aldrich Co. Ultrapure water (resistivity: $\rho \geq 18$ MΩ cm^{-1}) was used throughout all experiments.

1.2 Preparation of CeO_2 nanorods

The CeO_2 nanorods were synthesized using a solvothermal method. Typically, 3.48 g $Ce(NO_3)_3 \cdot 6H_2O$ and 19.2 g NaOH solid were dissolved in 40 mL ultrapure water, respectively. Then, NaOH solution was added into the $Ce(NO_3)_3 \cdot 6H_2O$ solution drop wisely under continuous stirring. After stirring at room temperature for 30 min, it was transferred into a 100 mL stainless steel vessel autoclave and kept at 100 °C for 24 h. After cooling down, the yellow powder was obtained by centrifugation and washed with water several times. The obtained CeO_2 precursor was dried in a vacuum oven at 60 °C for 12 h and then calcined at 500 °C for 3 h under the air atmosphere.

1.3 Preparation of CeF_3/CeO_2 and CeF_3

Typically, a certain amount of NH_4F and CeO_2 were loaded on the upstream and downstream respectively in a ceramic boat at a ratio of 2:1. The ceramic boat was then put into a tube furnace and calcined at 250 °C for 2 h under N_2 protection. After cooling down to room temperature, the final product was collected and named CeF_3/CeO_2. The CeF_3 support was prepared by a similar method by adjusting the raw material proportion to 4:1. It was worth noting that the contents of CeF_3 in the catalyst might be regulated by changing the amount of NH_4F, while due to the uncontrollable decomposition process, the final results can be not well controlled. While to our research, more CeF_3 will cause lower performance due to the bad conductivity and the easy dissolution of the CeF_3.

1.4 Preparation of Pd-CeO_2, Pd-CeF_3 and Pd-CeF_3/CeO_2

H_2PdCl_4 solution was prepared as follows. 0.05 M HCl diluted from concentrated hydrochloride acid was dropped into a certain amount of $PdCl_2$ at room temperature constantly in a water bath until the complete dissolution of $PdCl_2$.

The Pd particles supported on the as-prepared support were synthesized through a microwave-assisted reduction method. 34 mg CeO_2 rod, CeF_3, and CeF_3/CeO_2 were dispersed homogeneously into 50 mL ethylene glycol respectively by sonication. Then, a 567 μL diluted H_2PdCl_4 (30 mg mL^{-1}) solution was added to the suspension under continuous magnetic stirring. The pH value of the obtained mixture was adjusted to 11 by adding 1 M NaOH drop wisely. After that, the suspension was transferred into a 100 mL vial and placed in the middle of the microwave oven. It was then operated at 700 W for the 60 s on and 30 s off three times. When it came to room temperature, the mixture solution was filtrated and washed with DI water several times. After drying at 70 ^oC in a vacuum oven for 12 h, the final products were denoted as Pd-CeO_2, Pd-CeF_3, and Pd-CeF_3/CeO_2 separately. For a valid comparison, a homemade Pd/C catalyst of 20 wt.% was also prepared by the same approach.

1.5 Physical characterizations

Powder X-ray diffraction (XRD) patterns were recorded on a Bruker D8 Advance powder X-ray diffractometer using a Cu Kα (λ = 1.5405 Å) radiation source operating at 40 kV and 40 mA. Transmission electron microscopy (TEM) and element mapping analysis were conducted on a TECNAI G2 equipped with energy-dispersive X-ray, operated at 200 kV. Catalysts were sonicated and dispersed in ethanol before being placed onto a copper support grid for TEM observation. X-ray photoelectron spectroscopy (XPS) measurements were carried out using an ESCALAB250Xi spectrometer with an Al Kα radiation source. The XPS spectra were analyzed by XPSPEAK software.

1.6 Electrochemical measurements

All the electrochemical measurements were carried out in a conventional three-electrode electrochemical cell by Bio-logic SAS (France). The saturated calomel electrode (SCE, Hg/Hg_2Cl_2) was used as the reference electrode. All of the potentials are relative to the SCE electrode. A graphite rod and glassy carbon electrode (diameter d = 3 mm) were used as the counter and working electrode. For catalyst ink preparation, 3 mg catalyst and 2 mg Vulcan XC-72 carbon black were dispersed into 950 μL ethanol. Then, 50 μL 5 wt.% Nafion solution was added followed by sonication for at least 30 min

to form a homogeneous ink. 10 μL of the catalyst ink was loaded onto a pre-cleaned working electrode. The glassy carbon electrode was polished and thoroughly cleaned with an alumina slurry of 0.05 μm beforehand. For all experiments, the metal loading on the working electrode was maintained at 0.08 mg cm^{-2}.

Cyclic voltammetry was carried out at room temperature in 0.5 M H_2SO_4 containing 0.5 M HCOOH solution at a potential range between -0.2 and 1 V (vs SCE). The electrochemical impedance spectra (EIS) were recorded at the frequency range from 1000 kHz to 10 mHz with 12 points per decade. The amplitude of the sinusoidal potential signal was 5 mV. CO stripping voltammetry was measured in a 0.5 M H_2SO_4 solution. CO was purged into the H_2SO_4 solution for 15 min to allow the complete adsorption of CO onto the catalyst when the working electrode was kept at 0 V, and then excess CO in the electrolyte was purged out with N_2 for 15 min. The amount of CO was evaluated by the integration of the CO stripping peak, assuming 420 μC cm^{-2} of the coulombic charge required for the oxidation of the CO monolayer.

1.7 Electrochemical analysis

The activity of metal nanoparticles for formic acid electro-oxidation was measured. Before electrochemical measurements, a nitrogen flow was bubbled into the test system to remove the oxygen and the ad/desorption of hydrogen on metal nanoparticles surface was evaluated in 0.5 M H_2SO_4. Cyclic voltammetry was carried out at room temperature in 0.5 M H_2SO_4 and 0.5 M HCOOH mixture solution at a potential range between -0.2 and 1 V vs. SCE and at 50 mV s^{-1}.

The chronoamperometry (CA) experiments were performed in 0.5 M H_2SO_4 and 0.5 M HCOOH mixture solution at 0.1 V vs. SCE for 3600 s to estimate the stability of the catalysts for formic acid oxidation.

For formic acid oxidation, 99.99 % CO was subsequently bubbled in the 0.5 M H_2SO_4 for 15 min when the potential was controlled to be 0 V vs. SCE. The excess CO in the electrolyte was purged out with N_2 for 15 min. The CO stripping was performed in the potential of the range -0.2 ~ 1.0 V vs. SCE at a scan rate of 20 mV s^{-1}. The electrochemical surface areas (ECSA) and the tolerance to CO poisoning were estimated by the CO stripping test.

The electrochemical surface area (ECSA) values were calculated from the equation: ECSA=Q/Sl, where Q is the coulombic charge (in mC) obtained from the CO stripping curve. l is the loading of Pt on the surface of the electrode (in mg) and S is a proportionality constant of 420 μC cm^{-2}.

For the Tafel equation, $\eta = a + b\log(j)$, where η is the overpotential and j is the current density. The electrochemical impedance spectra (EIS) were recorded at the frequency range from 1000 kHz to 30 mHz with 12 points per decade. The amplitude of the sinusoidal potential signal was 5 mV.

2. Supporting Figures and Tables

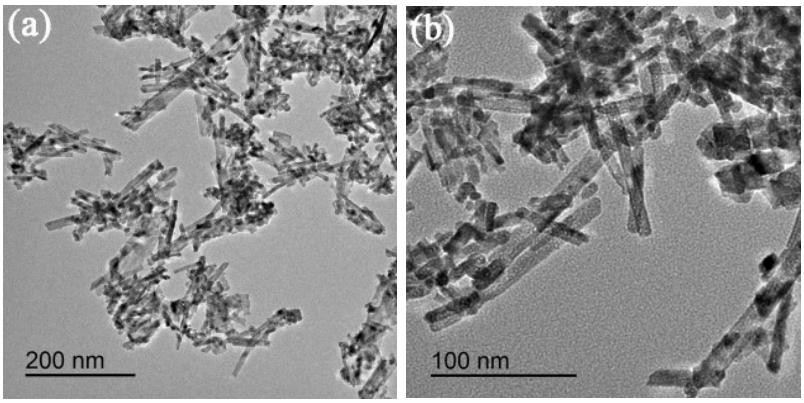

Figure S1. (a-b) TEM images of the CeO_2 nanorods.

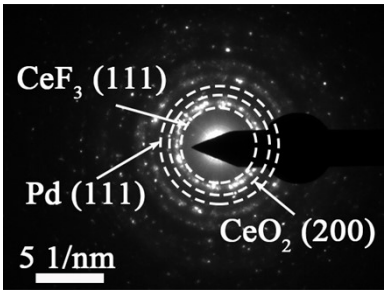

Figure S2. SAED pattern of Pd-CeF_3/CeO_2.

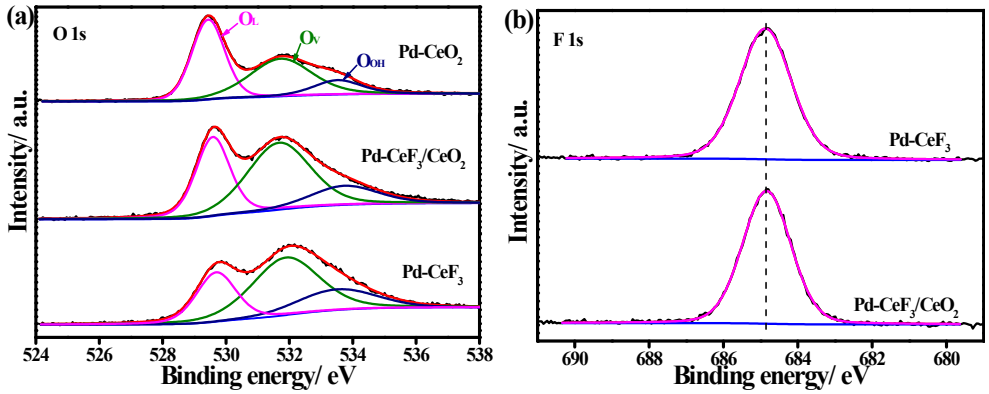

Figure S3. XPS spectra of (a) O 1s and (b) F 1s for corresponding catalysts.

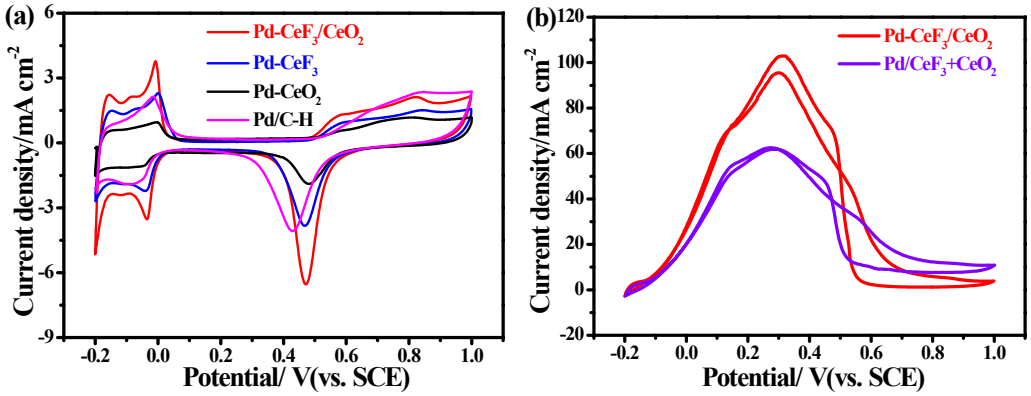

Figure S4. (a) Cyclic voltammograms of Pd-CeF_3/CeO_2, Pd-CeF_3, Pd-CeO_2 and Pd/C-H in 0.5 M H_2SO_4 at 50 mV s^{-1}. (b) Comparison of formic acid oxidation performance of Pd-CeF_3/CeO_2 and Pd/CeF_3+CeO_2 catalysts.

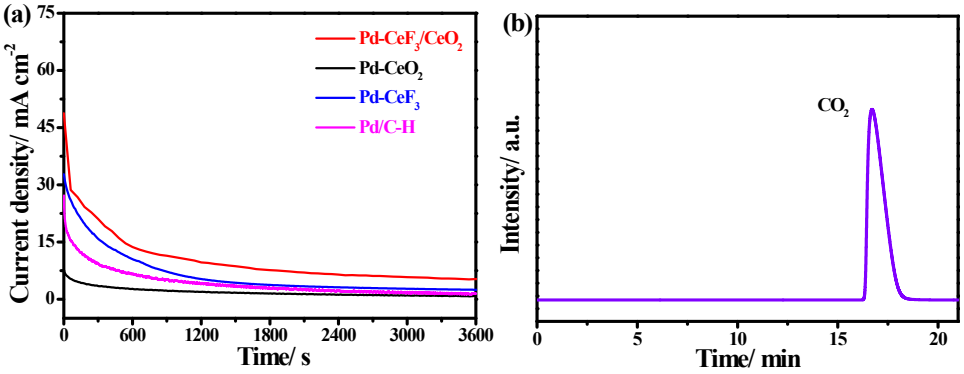

Figure S5. (a) Chronoamperometric curves of Pd-CeF_3/CeO_2, Pd-CeF_3, Pd-CeO_2 and Pd/C-H catalysts. (b) The gas chromatography spectrum of formic acid oxidation product of Pd-CeF_3/CeO_2.

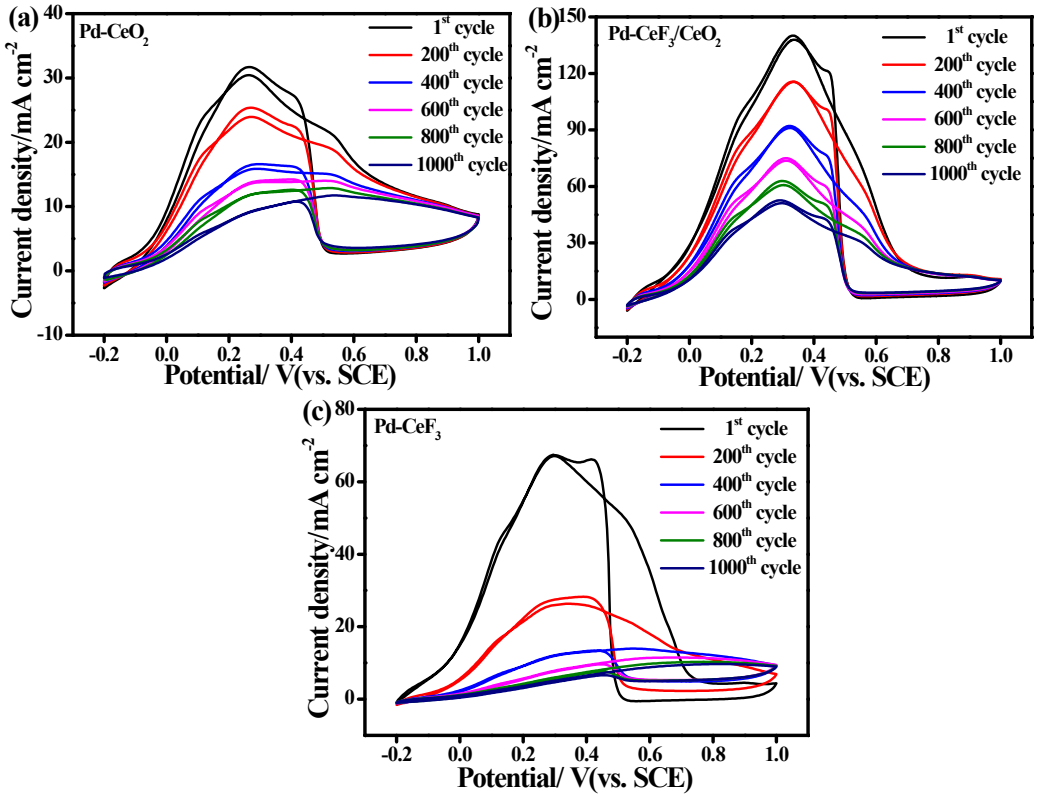

Figure S6. Dynamic stability by accelerated stability test on (a) Pd-CeO_2, (b) Pd-CeF_3/CeO_2, (c) Pd-CeF_3 catalysts in N_2-saturated 0.5 M H_2SO_4 containing 0.5 M HCOOH at 150 mV s^{-1}.

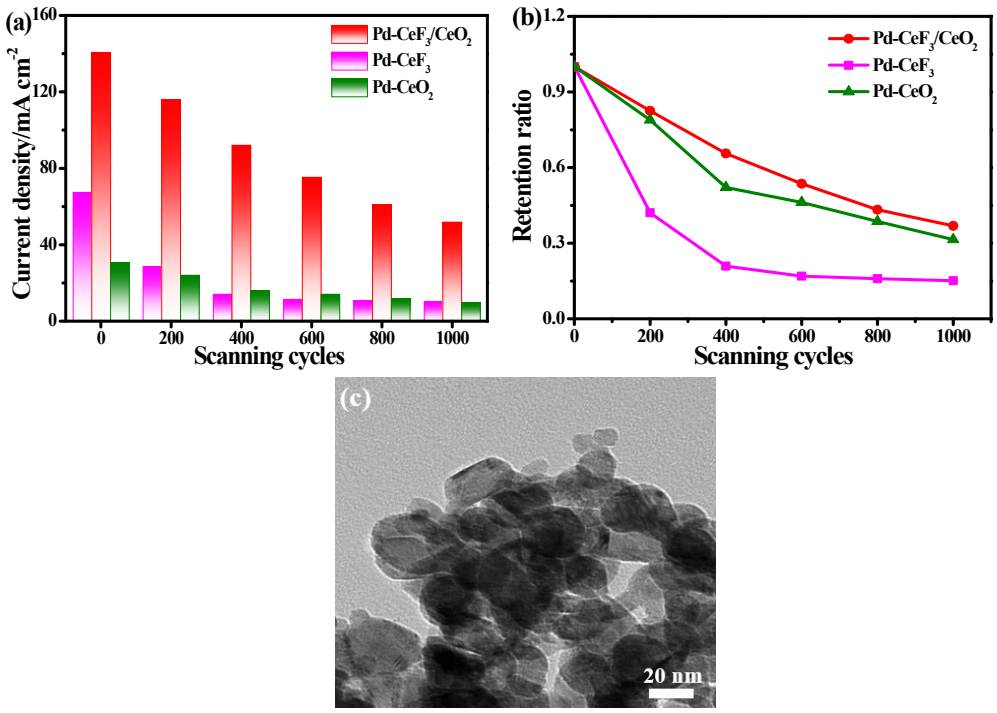

Figure S7. (a) Peak current density versus the scanning cycles of the corresponding catalysts for formic acid oxidation. (b) Normalized peak current density versus the scanning cycles for all the catalysts. (c) TEM image of Pd-CeF_3/CeO_2 after stability test of formic acid oxidation.

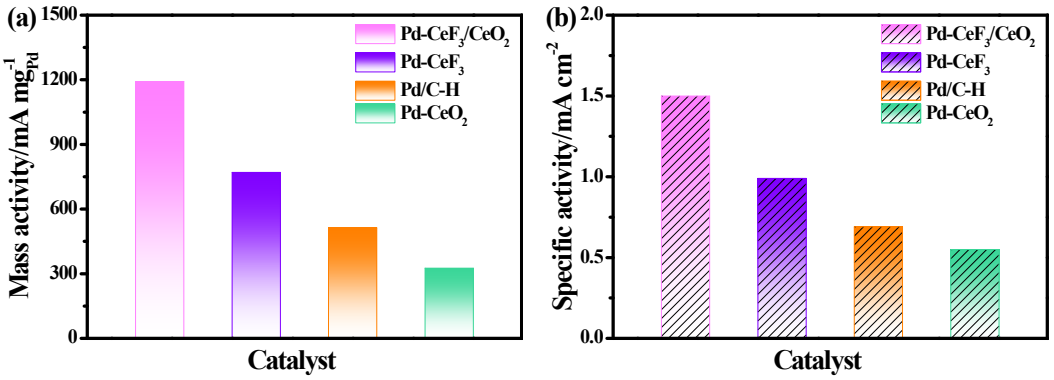

Figure S8. Mass activity and specific activity of Pd-CeF_3/CeO_2, Pd-CeF_3, Pd-CeO_2 and Pd/C-H catalysts.

Table S1. Relative content of different components for Pd-CeO_2, Pd-CeF_3/CeO_2 and Pd-CeF_3 catalysts from XPS analysis.

Catalysts	**Ce^{3+}/ %**	**Ce^{4+}/ %**	**O_V/ %**	**O_{OH}/ %**
Pd-CeO_2	20.2	79.8	42.8	13.7
Pd-CeF_3/CeO_2	60.6	39.4	44.3	27.6
Pd-CeF_3	73.2	26.8	45.1	30.7

Table S2. Relative content of Pd^0, PdO_x and PdO for Pd-CeO_2, Pd-CeF_3/CeO_2 and Pd-CeF_3 catalysts from XPS analysis.

Catalysts	**Pd^0/ %**	**PdO_x/ %**	**PdO/ %**
Pd-CeO_2	59.57	18.74	21.69
Pd-CeF_3/CeO_2	39.07	31.37	29.56
Pd-CeF_3	47.09	25.48	27.43

Table S3. EIS fitting parameters from equivalent circuits for different catalyst samples.

Catalysts	L / H	R_S / Ω	C / F	R_{ct} / Ω	CPE-Yo/S s^{-n}	CPE-n	R_0 / Ω
Pd-CeO_2	9.221E-9	7.281	1.589E-4	273.2	9.471E-4	0.7063	44.36
Pd-CeF_3	1.876E-6	6.913	6.447E-5	86.9	1.073E-3	0.6626	10.75
Pd-CeF_3/CeO_2	3.429E-9	6.052	1.450E-4	56.8	1.263E-3	0.6946	3.176
Pd/C-H	5.681E-8	8.071	1.390E-4	186.5	1.103E-3	0.7116	4.338

Table S4. Electrochemical surface area (ECSA) of different catalysts in 0.5 M H_2SO_4 estimated from CO stripping tests and the onset potential and CO oxidation peak potential for CO stripping.

Catalysts	**ECSA / m^2 g_{Pd}^{-1}**	**Onset potential / V vs. SCE**	**Peak potential / V vs. SCE**
Pd-CeO_2	33.6	0.65	0.69
Pd-CeF_3	43.7	0.61	0.66
Pd-CeF_3/CeO_2	44.8	0.60	0.64
Pd/C-H	41.9	0.67	0.71

Table S5. Comparisons of activities of various electrocatalysts for formic acid oxidation reaction.

Catalysts	Mass activity /mA mg^{-1}_{Pd}	Electrolyte	References
Pd-CeF_3/CeO_2	1192	0.5M H_2SO_4 + 0.5M HCOOH	This work
Pd/SnO_2/C	1000.5	0.5M H_2SO_4 + 0.5M HCOOH	[1]
Pd_3P PNTs	360.2	0.5M H_2SO_4 + 0.5M HCOOH	[2]
$TNP_{6.67}$@RFC@Pd_1	905	0.5M H_2SO_4 + 0.5M HCOOH	[3]
Pd/N-CQDs-SiO_2-rGO	951.4	0.5M H_2SO_4 + 0.5M HCOOH	[4]
Pd_4Sn NCNs	850.47	0.5M H_2SO_4 + 0.5M HCOOH	[5]
Pd_6Ga_4/rGO	762	0.5M H_2SO_4 + 0.5M HCOOH	[6]
Pd_3Cu/C-CeO_2	777.68	0.5M H_2SO_4 + 0.5M HCOOH	[7]
Pd/C-0.22EDA	1021	0.5M H_2SO_4 + 0.5M HCOOH	[8]
Pd-2.5 M	677.2	0.5M H_2SO_4 + 0.5M HCOOH	[9]

References

1 J. Wang, M. Feng, S. Hu and X. Zhang, *Int. J. Hydrogen Energy*, 2023, **48**, 15492-15503.

2 T. Wang, Y. Jiang, J. He, F. Li, Y. Ding, P. Chen and Y. Chen, *Carbon Energy*, 2022, **4**, 283-293.

3 G. Luo, S. Hu, D. Niu, S. Sun and X. Zhang, *Nanoscale*, 2022, **14**, 6007-6020.

4 S. Saipanya, P. Waenkaew, S. Maturost, N. Pongpichayakul, N. Promsawan, S. Kuimalee, O. Namsar, K. Income, B. Kuntalue, S. Themsirimongkon and J. Jakmunee, *ACS Omega*, 2022, **7**, 17741-17755.

5 Y. Gong, X. Liu, Y. Gong, D. Wu, B. Xu, L. Bi, L. Y. Zhang and X. S. Zhao, *J. Colloid Interface Sci.*, 2018, **530**, 189-195.

6 M. Sofian, F. Nasim, H. Ali, F. K. Kanodarwala and M. A. Nadeem, *Int. J. Hydrogen Energy*, 2024, **51**, 1277-1285.

7 C. Goswami, B. J. Borah, R. Das, K. Tada, S. Tanaka, I. P. Prosvirin, I. Z. Ismagilov, E. V. Matus, M. Kerzhentsev and P. Bharali, *J. Alloys Compd.*, 2023, **948**, 169665.

8 J. Li, Y. Jiang, J. Li, Y. Hu, Y. Shen, H. Zhao, Y. Zhu, Y. Zheng and H. Shao, *Int. J. Hydrogen Energy*, 2024, **78**, 1070-1077.

9 Y. Li, Y. Yan, M.-S. Yao, F. Wang, Y. Li, S. M. Collins, Y.-L. Chiu and S. Du, *Chem. Eng. J.*, 2023, **462**, 142244.